

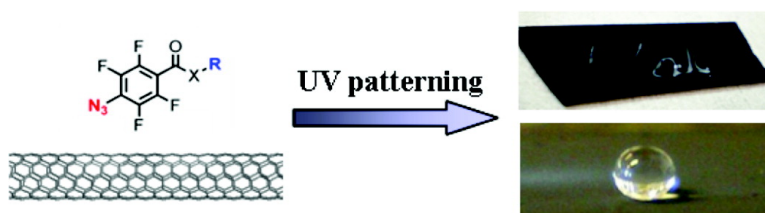
Communication

## A Facile and Patternable Method for the Surface Modification of Carbon Nanotube Forests Using Perfluoroarylazides

Stefan J. Pastine, David Okawa, Brian Kessler, Marco Rolandi, Mark Llorente, Alex Zettl, and Jean M. J. Frchet

*J. Am. Chem. Soc.*, **2008**, 130 (13), 4238-4239 • DOI: 10.1021/ja8003446

Downloaded from <http://pubs.acs.org> on February 8, 2009



### More About This Article

Additional resources and features associated with this article are available within the HTML version:

- Supporting Information
- Links to the 2 articles that cite this article, as of the time of this article download
- Access to high resolution figures
- Links to articles and content related to this article
- Copyright permission to reproduce figures and/or text from this article

[View the Full Text HTML](#)

## A Facile and Patternable Method for the Surface Modification of Carbon Nanotube Forests Using Perfluoroarylazides

Stefan J. Pastine,<sup>†</sup> David Okawa,<sup>†,§</sup> Brian Kessler,<sup>§</sup> Marco Rolandi,<sup>†,‡</sup> Mark Llorente,<sup>§</sup>  
Alex Zettl,<sup>§,‡</sup> and Jean M. J. Fréchet<sup>\*,†,‡</sup>

College of Chemistry and Department of Physics, University of California, Berkeley, California 94720-1460, and  
Materials Sciences Division, Lawrence Berkeley National Laboratory, Berkeley, California 94720

Received January 15, 2008; E-mail: frchet@berkeley.edu

In nature, a specific function is often provided by a unique combination of surface roughness and chemical composition. Preeminent examples include the Lotus leaf, the Water Strider leg, and the Gecko foot. The chemical vapor deposition (CVD) of arrays of vertically aligned carbon nanotubes (CNTs) provides a direct means to confer microscale structure with inherent nanoscale roughness to a surface (Figure 1). Hierarchical roughness and the possibility for chemical functionalization make nanotube forests attractive scaffolds for the fabrication of new materials. However, in order to realize the potential of this biomimetic approach, two issues need to be addressed: (1) the durability of nanotube forests is typically low; and (2) a facile method for chemical patterning of forests is lacking. Herein we describe a simple scheme for patterning robust CNT forests.

The structural integrity of vertical nanotube surfaces has been limited by weak adhesion of the film to the substrate and the propensity for film deformation upon solvent exposure due to strong van der Waals forces between tubes.<sup>1</sup> We addressed this issue by synthesizing multiwalled carbon nanotube (MWCNT) forests via a modified CVD technique.<sup>2</sup> To increase forest adhesion to the substrate, 10 nm thick iron catalyst films and a high ethylene concentration were used during growth. Specifically, flowing pure ethylene at 200 sccm for 10 min at a growth temperature of 750 °C resulted in forests with an average nanotube diameter of approximately 40 nm. Importantly, the as-grown forests were resistant to deformation by strong solvent streams and significant mechanical pressure/scratching. We believe that the observed durability stems from a cementing effect caused by amorphous carbon deposited on the nanotube surface during growth.

To develop a chemical patterning method, we investigated nitrene insertion into CNTs. Nitrenes have been used for the covalent modification of single-wall CNTs (SWCNTs) and MWCNTs.<sup>3,4</sup> Generation of nitrenes by photolytic decomposition of azides provided an opportunity for modifying forests in a spatially controlled manner. With this in mind, generic perfluoroarylazide **1** was selected as a scaffold for displaying molecular information on the surface of the nanotubes (Figure 2). The perfluoroarylazide moiety was selected as the nitrene precursor because of its high intermolecular insertion efficiency relative to other aryl- or alkylazides.<sup>5</sup> Furthermore, the specific azide chosen has a carboxyl group through which a variety of functionality can be attached via standard coupling reactions. It was envisioned that the R group in **1** could be used to tailor the surface properties, and that patterning could be achieved via exposure through a photomask.

To test if the azide side chain can modify surface properties, model compounds **2** and **3** were prepared. The hydroxyl-containing **2** and the fluoroalkyl-containing **3** were designed to control the

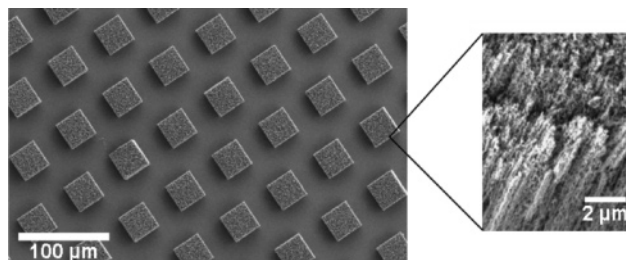


**Figure 1.** Patterned arrays of CNT forests provide both micro- and nanoscale structure to a substrate.

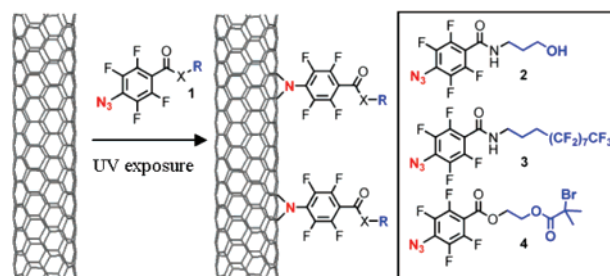


**Figure 2.** Perfluoroazides employed to modify CNT forests.

surface energy of the forests. The wetting behavior of a surface is dictated by a combination of surface roughness and chemical composition. Both superhydrophobic surfaces (contact angle (CA) > 150°; sliding angle < 5°) and superhydrophilic surfaces (CA near 0°) have aroused great interest for potential practical applications such as self-cleaning windows and stain resistant textiles.<sup>6</sup> Due to the nanoscale roughness of the template, attachment of **2** was expected to confer superhydrophilic properties to the substrate, while **3** was expected to confer superhydrophobic properties. As a basic procedure, substrates were dipped in a solution of azide in acetone (10 mg/mL), allowed to dry, exposed to UV radiation ( $\lambda = 254$  nm) for 5 min, and then rinsed by an acetone stream. Forests treated with **2** exhibited “sponge-like” behavior after UV exposure, with a water contact angle diminishing to nearly 0° after a few seconds. In stark contrast, forests treated with **3** exhibited superhydrophobic behavior; water droplets had nearly a spherical shape and were unstable on the surface due to the small hysteresis between the advancing and receding CAs ( $\theta_A/\theta_R = 162^\circ/161^\circ$ ).<sup>7</sup>

Having demonstrated that azides **2** and **3** can transform the properties of nanotube forests, we next turned our attention to azide **4**. The 2-bromoisobutyrate moiety in **4** serves as an initiator for atom transfer radical polymerization (ATRP)<sup>8</sup> and enables the grafting of a variety of polymers. UV-triggered attachment of **4** followed by polymerization of *N*-isopropylacrylamide (NIPAAm) under ATRP conditions resulted in modification of the forest surface with poly-NIPAAm.<sup>9</sup> Fourier transform infrared spectroscopy (FTIR) confirmed the presence of poly-NIPAAm on the substrate.

<sup>†</sup> College of Chemistry, University of California, Berkeley.

<sup>§</sup> Department of Physics, University of California, Berkeley.

<sup>‡</sup> Lawrence Berkeley National Laboratory.

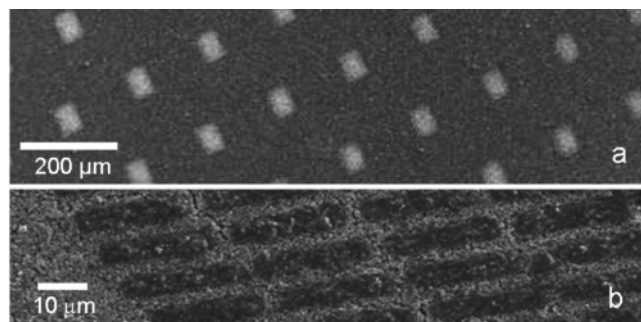


**Figure 3.** Scanning electron micrographs of poly-NIPAAm patterned on MWNT forests via polymerization initiator azide **4**. Dark areas represent polymer region. (a) Polymerized background with isolated unmodified regions. (b) Unmodified background with patterned regions of polymer.

To determine if modification was a result of grafting from the nanotube surface, a forest was coated in **4** and half of the substrate was masked during UV exposure. In contrast to the exposed region, no distinctive signals were observed in the FTIR spectrum of the masked region. Furthermore, no polymer decomposition was observed by thermogravimetric analysis (see Supporting Information). These results indicated that a surface-initiated polymerization was enabled by the phototriggered attachment of azide initiator **4**. Using appropriate photomasks, we prepared substrates with isolated polymerized features as small as  $5\ \mu\text{m}$ , as well as a polymerized background with isolated pristine regions as small as  $60\ \mu\text{m}$  (Figure 3).

The exact site of functionalization had to be clarified because of the likely presence of amorphous carbon on the forest substrates. To ensure that CNTs can be functionalized under our treatment conditions, we prepared bucky paper from HiPCO SWCNTs. The static CA of the paper increased from  $68$  to  $110^\circ$  after treatment with **3**. Further evidence for covalent attachment was provided by Raman spectroscopy. After modification, an increase in the D band intensity ( $I_D$ ) occurred with a concomitant decrease in the G band intensity ( $I_G$ ) (see Supporting Information). The observed increase in the  $I_D/I_G$  ratio is indicative of an incorporation of defect sites in the nanotube lattice.<sup>3</sup> A second treatment with **3** resulted in a further increase in the  $I_D/I_G$  ratio, indicating that additional modification of the substrate occurred.

The ability to increase the extent of functionalization by a second treatment suggested that different azides could be used to further tailor or alter the surface properties of forest substrates. This was demonstrated by reversal of the surface energy of a forest template. Superhydrophilic samples produced after modification with **2** became superhydrophobic by a subsequent treatment with **3**. This overriding of hydrophilicity is attributed to the significantly longer length of the fluoroalkyl chain in **3**, relative to the hydroxyl chain in **2**. Considerable attention has been paid to developing surfaces with differential wettability.<sup>10</sup> However, only a few examples of stable patterned superhydrophilic–superhydrophobic surfaces have been reported.<sup>11</sup> The ability of **3** to override **2** allowed the fabrication of superhydrophobic substrates with hydrophilic regions in two simple steps: (i) blanket modification with **2**; and (ii) treatment with **3** followed by irradiation through an appropriate photomask. Figure 4a demonstrates the wetting characteristics of a prepared macrochannel. Water was effectively confined to the hydrophilic region of the substrate by the superhydrophobic background. Droplets that landed on the superhydrophobic region rolled either off the substrate or into the hydrophilic channel. The macropatterned films remained stable for at least 1 month. A micropatterned substrate was also prepared using a quartz mask with  $80\ \mu\text{m}$  squares. A microdroplet array was produced from selective condensation of water vapor in the hydrophilic regions of the surface (Figure

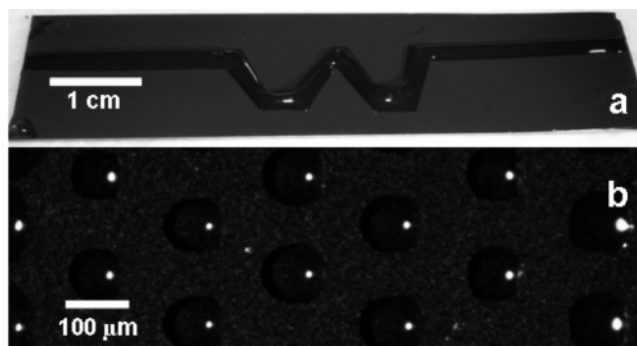


**Figure 4.** Superhydrophilic patterns on superhydrophobic backgrounds: (a) a macrochannel. (b) Dark field image of selective condensation on micropatterned hydrophilic regions.

4b). This specialized surface effectively serves as a synthetic mimic to the back of the *Stenocara* beetle of the Namib desert.<sup>12</sup> To the best of our knowledge, this is the first demonstration of a stable superhydrophobic surface with hydrophilic features of less than  $100\ \mu\text{m}$ .

In conclusion, we have developed a simple patterning method for the functionalization of CNT forests. The nanoscale roughness of the forest template was utilized to make superhydrophilic patterns on a superhydrophobic background. Ongoing work in our laboratories is directed toward fabricating advanced materials by coupling the optical and/or electrical properties of aligned CNTs to chemical modification.

**Acknowledgment.** The authors acknowledge financial support from the Office of Basic Energy Sciences, Division of Materials Sciences and Engineering, of the U.S. Department of Energy contract DE-AC02-05CH11231. We thank NIH (fellowship to S.J.P.), Intel (fellowship to M.R.), DOD (NDSEG fellowship to B.K.) and the Miller Foundation for a Miller Professorship to A.Z.

**Supporting Information Available:** Experimental procedures and spectroscopic data for starting materials and products. This material is available free of charge via the Internet at <http://pubs.acs.org>.

## References

- (1) (a) Watts, P. C. P.; Lyth, S. M.; Mendoza, E.; Silva, S. R. P. *Appl. Phys. Lett.* **2006**, *89*, 103113. (b) Chakrapani, N.; Wei, B.; Carrillo, A.; Ajayan, P. M.; Kane, R. S. *Proc. Natl. Acad. Sci. U.S.A.* **2004**, *101*, 4009–4012.
- (2) Wang, K.; Dai, H.; Fishman, H. A.; Harris, J. S. *Proc. SPIE* **2005**, *5718*, 22–29.
- (3) (a) Holzinger, M.; Abraham, J.; Whelan, P.; Graupner, R.; Ley, L.; Hennrich, F.; Kappes, M.; Hirsch, A. *J. Am. Chem. Soc.* **2003**, *125*, 8566–8580. (b) Holzinger, M.; Vostrowsky, O.; Hirsch, A.; Hennrich, F.; Kappes, M.; Weiss, R.; Jellen, F. *Angew. Chem., Int. Ed.* **2001**, *40*, 4002–4005.
- (4) (a) Moghaddam, M. J.; Taylor, S.; Gao, M.; Huang, S.; Dai, L.; McCall, M. J. *Nano Lett.* **2004**, *4*, 89–93. (b) Lee, K. M.; Li, L.; Dai, L. *J. Am. Chem. Soc.* **2005**, *127*, 4122–4123.
- (5) (a) Keana, J. F. W.; Cai, S. J. X. *J. Org. Chem.* **1990**, *55*, 3640–3647. (b) Cai, S. X.; Nabity, J. C.; Wybourne, M. N.; Keana, J. F. W. *Chem. Mater.* **1990**, *2*, 631–633.
- (6) Feng, X.; Jiang, L. *Adv. Mater.* **2006**, *18*, 3063–3068.
- (7) (a) Lau, K. K. S.; Bico, J.; Teo, K. B. K.; Chhowalla, M.; Amarantunga, G. A. J.; Milne, W. I.; McKinley, G. H.; Gleason, K. K. *Nano Lett.* **2003**, *3*, 1701–1705. (b) Li, H.; Wang, X.; Song, Y.; Liu, Y.; Li, Q.; Jiang, L.; Zhu, D. *Angew. Chem., Int. Ed.* **2001**, *40*, 1743–1746.
- (8) Matyjaszewski, K.; Xia, J. *Chem. Rev.* **2001**, *101*, 2921–2990.
- (9) Sun, T.; Liu, H.; Song, W.; Wang, X.; Jiang, L.; Zhu, D. *Angew. Chem., Int. Ed.* **2004**, *43*, 4663–4666.
- (10) Representative examples: (a) Lopez, G. P.; Biebuyck, H. A.; Frisbie, C. D.; Whitesides, G. M. *Science* **1993**, *260*, 647–649. (b) Sun, T.; Wang, G.; Liu, H.; Feng, L.; Jiang, L.; Zhu, D. *J. Am. Chem. Soc.* **2003**, *125*, 14996–14997.
- (11) (a) Zhai, L.; Berg, M. C.; Cebeci, F. C.; Kim, Y.; Milwild, J. M.; Rubner, M. F.; Cohen, R. E. *Nano Lett.* **2006**, *6*, 1213–1217. (b) Garrod, R. P.; Harris, L. G.; Schofield, W. C. E.; McGettrick, J.; Ward, L. J.; Teare, D. O. H.; Badyal, J. P. S. *Langmuir* **2007**, *23*, 689–693.
- (12) Parker, A. R.; Lawrence, C. R. *Nature* **2001**, *414*, 33.

JA8003446